

On the dispersion relation for the kinetic Alfvén wave in an inhomogeneous plasma

Robert L. Lysak

School of Physics and Astronomy, University of Minnesota, Minneapolis, Minnesota 55455, USA

(Received 4 January 2008; accepted 3 April 2008; published online 3 June 2008)

The kinetic Alfvén wave has been recognized as an important wave mode in magnetospheric plasmas and laboratory plasmas, and has potential application in many areas of cosmic plasma physics. The kinetic dispersion relation of this mode has been described including finite frequency and finite ion gyroradius corrections. Laboratory plasmas as well as plasmas in space often contain strong gradients perpendicular to the background magnetic field. In this case, the dispersion relation must be generalized to include changes in the plasma parameters on each side of the gradient. In the presence of such gradients, localized modes can be found in the plasma. Depending on the relative values of the Alfvén speed and the plasma beta across these gradients, these modes can be trapped within the cavity or enhancement or propagate across the gradient. © 2008 American Institute of Physics. [DOI: 10.1063/1.2918742]

I. INTRODUCTION

Recent data from the FAST satellite has established that kinetic Alfvén waves play an important role in auroral particle acceleration.¹⁻⁴ Polar observations⁵⁻⁹ have shown that these waves carry significant Poynting flux toward the auroral ionosphere and show signatures of electron acceleration. These observations have confirmed theoretical work that has suggested such a connection over many years.¹⁰⁻¹² More recent theoretical work¹³⁻²² has given further details on the wave-particle interactions of kinetic Alfvén waves through test particle modeling as well as more self-consistent theories including the feedback of the hot electrons on the wave structure.

The importance of the kinetic Alfvén wave in space plasmas has led to laboratory investigations of the properties of this mode, notably in the Large Plasma Device (LAPD) at UCLA.²³ In this device, the structure of kinetic Alfvén waves can be diagnosed and compared with the dispersion relation for these waves.^{24,25} In the LAPD, the waves propagate in a long plasma column, and investigations of the propagation of waves in the presence of the perpendicular density gradients inherent in this configuration have been performed by Maggs and Morales.²⁶ In particular, the transition between the kinetic and inertial limits of the kinetic Alfvén wave dispersion relation has been investigated by Vincena *et al.*²⁷

Density cavities on a variety of scales are well known in the auroral acceleration region as well.^{1,28-31} These density cavities often occur above parallel electric field regions, with the cold ionospheric plasma becoming depleted and only warm plasma sheet plasma present. Thus, these cavities often have a higher temperature than the surrounding medium. Recently, Chaston *et al.*⁴ have studied such a cavity in detail and showed that it is associated with strong Alfvén wave activity, which evidently heats ions and ejects them to higher altitudes. These waves show the dispersion expected for kinetic Alfvén waves in the inertial regime, with their perpendicular group velocity opposite in direction to the perpendicular phase velocity.

Some studies have investigated the propagation of Alfvén waves in density cavities from a theory and modeling point of view. Rankin *et al.*^{32,33} considered low-frequency field line resonances and the self-consistent density cavities that were produced by the ponderomotive force of the wave. They considered the self-consistent evolution of low-frequency field line resonances and the corresponding mode structure including the perturbations in the density. Drozdenko and Morales³⁴ considered the propagation of a large-scale Alfvén wave through a density cavity with a perpendicular scale of the electron inertial length. The polarization current of such a wave acted as an antenna radiating Alfvén wave on the inertial scale. Génot *et al.*³⁵⁻³⁸ have developed an electromagnetic particle-in-cell code to investigate the propagation of Alfvén waves through a density cavity. They showed that the Alfvén wave quickly developed small scales and parallel electric fields on the gradient boundaries.

It is the purpose of this paper to investigate the properties of Alfvén waves in the presence of density cavities in light of both laboratory and space experiments. We will begin with a consideration of the dispersion relation of Alfvén waves in a uniform plasma at finite frequency, which is important in the laboratory and possibly in space. Secondly, the mode structure of Alfvén waves in a density cavity will be considered. In contrast to previous work that considered the self-consistent evolution of low-frequency wave structures,^{32,33} we will assume that the density cavity is given and consider waves with periods short compared to the time scales on which the density evolves. It will be seen that discrete modes of the kinetic Alfvén wave can exist in cavities that are larger than the dispersive scales in the plasma.

II. KINETIC ALFVÉN WAVE DISPERSION AT FINITE FREQUENCY

The full kinetic Alfvén wave dispersion relation in a uniform plasma has been given in a number of works, in particular Lysak and Lotko,¹⁵ who wrote this dispersion relation

in the low-frequency limit in terms of the dielectric tensor as

$$\det \begin{pmatrix} \epsilon_{\perp} - n_{\parallel}^2 & n_{\perp} n_{\parallel} \\ n_{\perp} n_{\parallel} & \epsilon_{\parallel} - n_{\perp}^2 \end{pmatrix} = 0, \quad (1)$$

where the dielectric tensor elements are

$$\epsilon_{\perp} = 1 + \frac{c^2}{V_A^2} \frac{1 - \Gamma_0(\mu_i)}{\mu_i}, \quad \epsilon_{\parallel} = 1 + \frac{\Gamma_0(\mu_e)}{k_{\parallel}^2 \lambda_D^2} [1 + \xi Z(\xi)], \quad (2)$$

where $\mu_{e,i} = k_{\perp}^2 \rho_{e,i}^2$, $\xi = \omega/k_{\parallel} a_e$, and Γ_0 and Z are the modified Bessel function and the plasma dispersion function, respectively. This equation can be solved numerically and the dispersion relation written in the form,

$$\left(\frac{\omega}{k_{\parallel} V_A} \right)^2 = \frac{1}{V_A^2/c^2 + [1 - \Gamma_0(\mu_i)]/\mu_i} + \frac{k_{\perp}^2 \rho_s^2}{\Gamma_0(\mu_e)[1 + \xi Z(\xi)] + k_{\parallel}^2 \lambda_D^2}, \quad (3)$$

where $\rho_s^2 = (T_e/T_i)\rho_i^2$ is the ion acoustic gyroradius. In many cases, Eq. (3) can be simplified by taking $V_A^2 \ll c^2$, $\mu_e \rightarrow 0$, and $k_{\parallel}^2 \lambda_D^2 \ll 1$ so that it becomes

$$\left(\frac{\omega}{k_{\parallel} V_A} \right)^2 = \frac{\mu_i}{1 - \Gamma_0(\mu_i)} + \frac{k_{\perp}^2 \rho_s^2}{1 + \xi Z(\xi)}. \quad (4)$$

Alternatively, this dispersion relation can be written in the form given by Gekelman *et al.*,²⁴ including a finite frequency correction,

$$\left(\frac{k_{\perp} c}{\omega_{pe}} \right)^2 = Z'(\xi) \left[\frac{V_A^2 \mu_i (1 - \omega^2/\Omega_i^2)}{a_e^2 (1 - \Gamma_0(\mu_i))} - \xi^2 \right], \quad (5)$$

where $Z'(\xi) = -2[1 + \xi Z(\xi)]$ is the derivative of the dispersion function. This form is exactly equivalent to Eq. (4) except for the frequency term.

The finite frequency correction can be found from the form given by Eq. (1) by noting that for the general Maxwellian distribution function, the dielectric tensor element is given by

$$\epsilon_{\perp} = 1 + \frac{\omega_{pi}^2}{\omega^2} \frac{\omega}{k_{\parallel} a_i} \sum_{n=-\infty}^{\infty} \frac{n^2 \Gamma_n(\mu)}{\mu} Z \left(\frac{\omega - n\Omega_i}{k_{\parallel} a_i} \right) \approx 1 + \frac{c^2}{V_A^2} G(\mu, \omega/\Omega_i). \quad (6)$$

The last form follows if we expand the Z functions for large argument, $|\omega - n\Omega_i|/k_{\parallel} a_i \gg 1$, which is valid for long-wavelength waves in a relatively cold ion plasma as long as the wave frequency is not too close to a harmonic of the ion gyrofrequency. In this case, the function G can be written as

$$G(\mu, \omega) = \sum_{n=1}^{\infty} \frac{2\Gamma_n(\mu)}{\mu} \frac{1}{1 - \omega^2/n^2\Omega_i^2}. \quad (7)$$

If the finite frequency term is neglected in all but the $n=1$ term, then G takes the form,

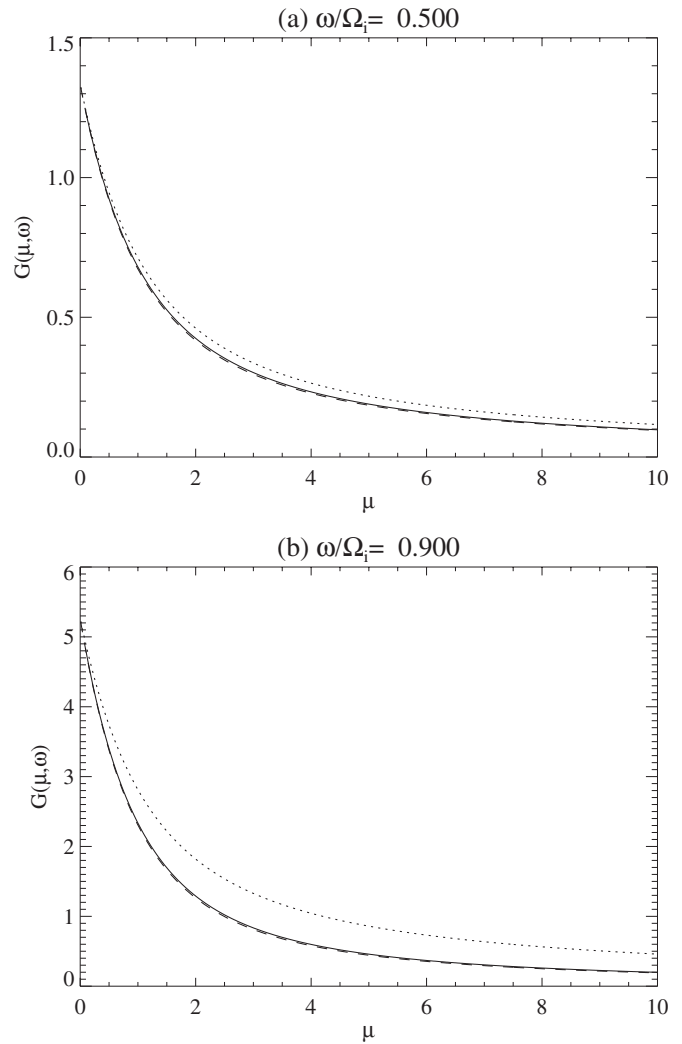


FIG. 1. Comparison of three forms for the ion gyroradius correction factor G for (a) $\omega/\Omega_i=0.5$ and (b) 0.9 . In each panel, the solid line is the exact expression (7) with 100 terms included, the dashed line is the approximation given by Eq. (8), and the dotted line is the approximation given by Eq. (11). It can be seen that while both approximations are reasonable, especially for lower frequency, the expression (8) gives quantitatively better results.

$$G(\mu, \omega/\Omega_i) = \frac{1 - \Gamma_0(\mu)}{\mu} + \frac{2\Gamma_1(\mu)}{\mu} \frac{\omega^2/\Omega_i^2}{1 - \omega^2/\Omega_i^2}. \quad (8)$$

With this expression we can write Eqs. (4) and (5), respectively, as

$$\left(\frac{\omega}{k_{\parallel} V_A} \right)^2 = \frac{1}{G(\mu_i, \omega/\Omega_i)} + \frac{k_{\perp}^2 \rho_s^2}{1 + \xi Z(\xi)} \quad (9)$$

or

$$\left(\frac{k_{\perp} c}{\omega_{pe}} \right)^2 = Z'(\xi) \left[\frac{V_A^2}{a_e^2} \frac{1}{G(\mu_i, \omega/\Omega_i)} - \xi^2 \right]. \quad (10)$$

Equation (5) therefore implies

$$G(\mu_i, \omega/\Omega_i) = \frac{1 - \Gamma_0(\mu_i)}{\mu_i (1 - \omega^2/\Omega_i^2)}. \quad (11)$$

Figure 1 shows the functional dependence of the different forms of G represented by Eqs. (7), (8), and (11) for ω/Ω_i

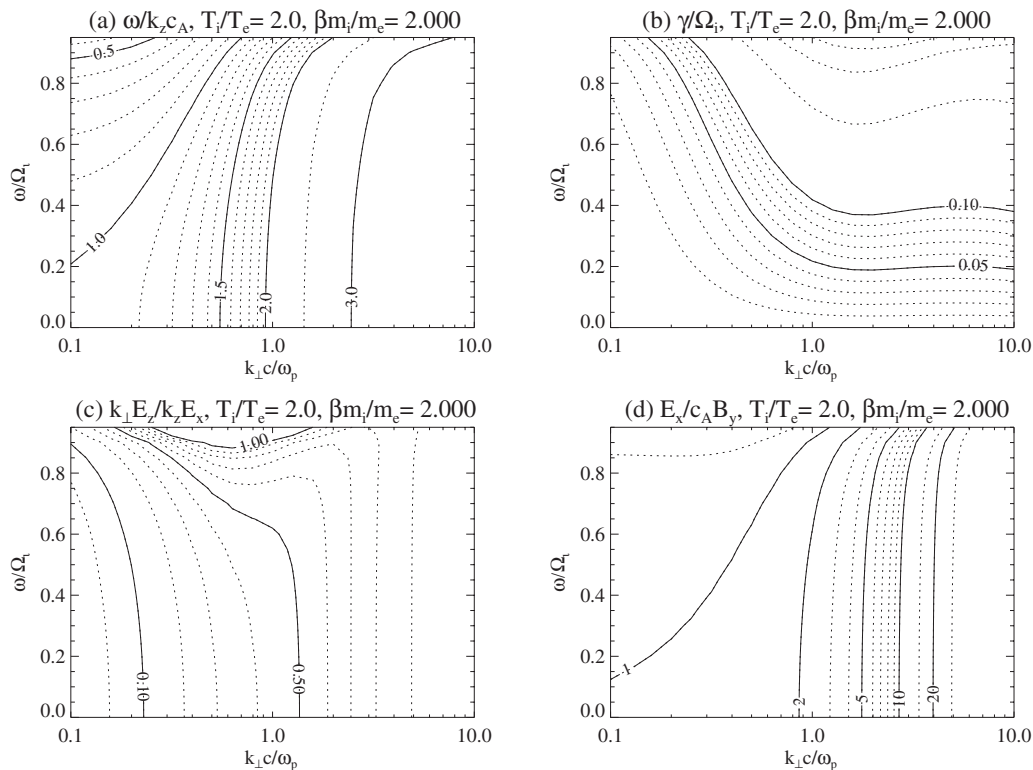


FIG. 2. Solutions to the dispersion relation as a function of frequency and perpendicular wave number for $T_i=2T_e$ and $\beta=2.0m_e/m_i$. (a) Parallel phase velocity normalized to Alfvén speed; (b) damping rate normalized to ion cyclotron frequency; (c) ratio of parallel to perpendicular electric fields, normalized by the ratio of perpendicular to parallel wavelength; (d) ratio of perpendicular electric and magnetic field components normalized to Alfvén speed.

$=0.5$ and 0.9 . It can be seen that these expressions are not too different, but noticeable differences between Eq. (11) and the full expression (7) occur, especially for higher frequency. In the following, we will use the more accurate approximation given by Eq. (8).

Figure 2 shows the solutions of Eq. (9) as a function of frequency and perpendicular wave number for the case where $\beta=2.0m_e/m_i$, which corresponds to $V_A^2/a_e^2=0.5$. The four plots in this figure show (a) the real parallel phase velocity normalized to the Alfvén speed; (b) the damping rate; (c) the ratio of the parallel to the perpendicular magnetic field, normalized to the ratio of the perpendicular and parallel wave numbers; and (d) the ratio of the perpendicular electric and magnetic fields, normalized to the Alfvén speed. It can be seen that for larger perpendicular wave numbers, the finite frequency correction is not too important, except for an increase in the damping rate. However, for smaller k_\perp , the finite frequency correction becomes important above about $\omega/\Omega_i \sim 0.2$. Similar results (not shown) indicate that as the β is lowered, the region in which the finite frequency correction is important expands.

As a test of this approximate dispersion relation, Fig. 3 shows the corresponding figures resulting from a run of the WHAMP code³⁹ which solves the full 3×3 dispersion relation including all harmonics. It can be seen that these figures agree in the regions where WHAMP finds a solution; the WHAMP code fails when the damping rate becomes too high. Thus, it can be seen that for $\omega < 0.9\Omega_i$, the approximate dispersion relation gives a reasonable result. In laboratory plasmas where $\omega/\Omega_i \sim 0.5$, the finite frequency effect is clearly

important. In the auroral zone, the ion gyrofrequency is about 100 Hz for protons at an altitude of $2R_E$ and 30 Hz for oxygen at an altitude of 1000 km, which is a typical oxygen scale height. Alfvén waves trapped in the ionospheric Alfvén resonator have frequencies up to about 1 Hz; thus, the finite frequency correction is less significant for this situation, although it may become important in cases where significant amounts of oxygen are present at higher altitudes.

III. ALFVÉN CAVITY MODES IN TRANSVERSE GRADIENTS

Next, consider the structure of Alfvén modes in a strong gradient in density transverse to a background magnetic field. The full kinetic description as described by Eq. (1) is generally difficult to apply in the strongly inhomogeneous case, however, and a fluid model is more applicable. To account for the cylindrical geometry of laboratory devices (and noting that density perturbations in the auroral plasma may also have a cylindrical topology), we will develop such a model in cylindrical coordinates, and for simplicity, will assume no azimuthal spatial dependence, i.e., $m=0$. In this case, the shear and compressional modes decouple and we can write the wave fields in terms of the radial electric field E_r , the azimuthal magnetic field B_ϕ , and the parallel electric field E_z . Assuming a dependence of $\exp(ik_\parallel z - i\omega t)$ but leaving the r dependence unspecified we can write Faraday's law as

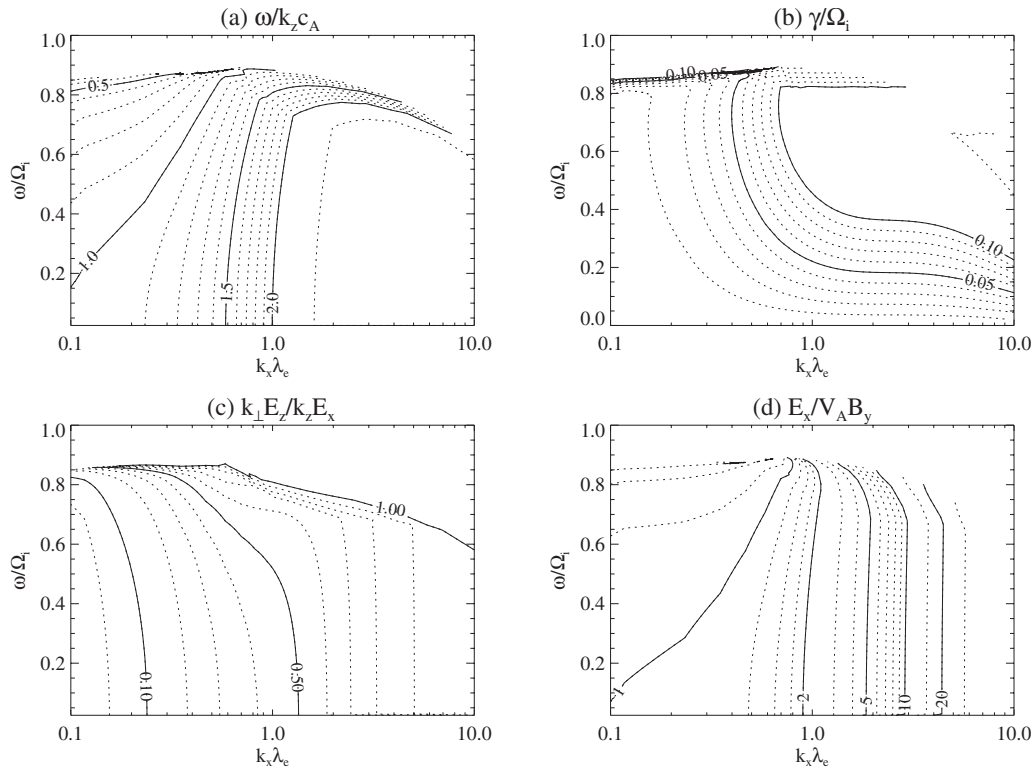


FIG. 3. Solutions from the full dispersion relation calculated using the WHAMP code. Panels (a)–(d) plot the same variables as in Fig. 2.

$$-i\omega B_\varphi = -ik_\parallel E_r + \frac{\partial E_z}{\partial r}. \quad (12)$$

The parallel current is assumed to be carried mainly by electrons, and the parallel equation of motion can be written in terms of the current as

$$-i\omega j_z = \frac{ne^2}{m_e} E_z + \frac{e}{m_e} ik_\parallel \delta p_e. \quad (13)$$

We will assume isothermal electrons and take $\delta p_e = T_e \delta n_e$, and using the continuity equation to eliminate δn_e we can write

$$\left(-i\omega + i\frac{k_\parallel^2 T_e}{\omega m_e}\right) j_z = \frac{ne^2}{m_e} E_z. \quad (14)$$

If we now write Ampere's law in cylindrical coordinates, we have

$$j_z = \frac{1}{\mu_0 r} \frac{\partial}{\partial r} (rB_\varphi). \quad (15)$$

Then we can write

$$E_z = -i\omega \lambda^2 \left(1 - \frac{k_\parallel^2 v_e^2}{\omega^2}\right) \frac{1}{r} \frac{\partial}{\partial r} (rB_\varphi), \quad (16)$$

where $\lambda^2 = m_e / \mu_0 n e^2$ is the square of the electron inertial length and $v_e^2 = T_e / m_e$ is the electron thermal speed. Since $\lambda^2 v_e^2 = V_A^2 \rho_s^2$, where ρ_s is the ion acoustic gyroradius defined above, Eq. (17) can be written as

$$E_z = -i\omega \left(\lambda^2 - \frac{k_\parallel^2 V_A^2}{\omega^2} \rho_s^2\right) \frac{1}{r} \frac{\partial}{\partial r} (rB_\varphi) = -i\omega \lambda'^2 \frac{1}{r} \frac{\partial}{\partial r} (rB_\varphi), \quad (17)$$

where we have introduced the notation $\lambda'^2 = \lambda^2 - (k_\parallel^2 V_A^2 / \omega^2) \rho_s^2$. If the full kinetic effects are included, the expression for the parallel electric field can be found directly from the dielectric tensor as given by Eq. (2). Noting that $\varepsilon_\parallel = \varepsilon_0(1 + i\sigma_\parallel / \omega \varepsilon_0)$, we can write the kinetic analog of Eq. (17) as

$$E_z = i\omega \rho_s^2 \left(\frac{k_\parallel V_A}{\omega}\right)^2 \frac{1}{1 + \xi Z(\xi)} \frac{1}{r} \frac{\partial}{\partial r} (rB_\varphi). \quad (18)$$

This expression gives the terms in Eq. (17) in the cold and hot plasma limits. Thus, we may redefine λ'^2 above in order to take the kinetic effects into account, although we will use the two-fluid result (17) in the expressions below.

Next we need an equation for the perpendicular electric field. In a cold plasma, this can be found through the expression for the polarization current,

$$j_r = \frac{1}{\mu_0 V_A^2} (-i\omega E_r) = \frac{1}{\mu_0} (ik_\parallel B_\varphi). \quad (19)$$

This can be generalized to include the finite ion gyroradius and finite gyrofrequency effects as in the first section of the paper, noting that the polarization current is related to the ε_\perp component of the dielectric tensor, implying that we can generalize Eq. (19) by writing

$$j_r = \frac{G(\mu, \omega/\Omega_i)}{\mu_0 V_A^2} (-i\omega E_r), \quad (20)$$

where G may take the forms described in Eqs. (7), (8), and (11), depending on the approximation employed. The difficulty is that μ is written in terms of the perpendicular wave number, which cannot be assumed to be fixed here. In this case, we can expand the electric field in a Taylor series around the guiding center position (see Appendix), which leads to

$$j_r = \frac{-i\omega}{\mu_0 V_A^2 (1 - \omega^2/\Omega_i^2)} \left(1 + \frac{3}{4} \frac{\rho_i^2}{1 - \omega^2/4\Omega_i^2} \nabla_\perp^2 \right) E_r. \quad (21)$$

Assuming that the gyroradius correction is small, we can rewrite Eq. (21) as

$$\begin{aligned} E_r &= \frac{i\mu_0 V_A^2 (1 - \omega^2/\Omega_i^2)}{\omega} \left(1 - \frac{3}{4} \frac{\rho_i^2}{1 - \omega^2/4\Omega_i^2} \nabla_\perp^2 \right) j_r \\ &= -\frac{k_\parallel V_A^2 (1 - \omega^2/\Omega_i^2)}{\omega} \left(1 - \frac{3}{4} \frac{\rho_i^2}{1 - \omega^2/4\Omega_i^2} \nabla_\perp^2 \right) B_\varphi. \end{aligned} \quad (22)$$

An alternative approximation can be found by utilizing the form (11) and employing the Padé approximation^{40,41} to write

$$\frac{1 - \Gamma_0(\mu)}{\mu} \approx \frac{1}{1 + \mu} = \frac{1}{1 + k_\perp^2 \rho_i^2}. \quad (23)$$

In this case the operator in Eq. (22) can be written as $(1 - \rho_i^2 \Delta_\perp^2) B_\varphi$. This form is a reasonable approximation to the Bessel function for all arguments μ ; however, the expression (22) is more accurate for small values of μ . In any case, the two forms can be reconciled by a small redefinition of the thermal ion gyroradius ρ_i . If we define the transverse Laplacian operator in cylindrical geometry by using the relationship

$$\kappa^2 = \frac{(k_\parallel^2 V_A^2 / \omega^2)(1 - \omega^2/\Omega_i^2) - 1}{\lambda^2 - (k_\parallel^2 V_A^2 / \omega^2) \rho_s^2 - (k_\parallel^2 V_A^2 / \omega^2)(3\rho_i^2/4)(1 - \omega^2/\Omega_i^2)/(1 - \omega^2/4\Omega_i^2)}. \quad (29)$$

If we neglect the ion gyrofrequency correction and combine the gyroradius terms, this can be more simply written as

$$\kappa^2 = \frac{k_\parallel^2 V_A^2 - \omega^2}{\omega^2 \lambda^2 - k_\parallel^2 V_A^2 \rho^2}, \quad (30)$$

where $\rho^2 = \rho_s^2 + \rho_i^2$. This expression just represents the perpendicular wave number in the dispersion relation for kinetic Alfvén waves in the two-fluid approximation,

$$\omega^2 = k_\parallel^2 V_A^2 \frac{1 + \kappa^2 \rho^2}{1 + \kappa^2 \lambda^2}. \quad (31)$$

The condition $\kappa^2 > 0$, indicating a propagating wave, corresponds to the limits

$$\nabla^2 \mathbf{V} = \nabla \nabla \cdot \mathbf{V} - \nabla \times (\nabla \times \mathbf{V}), \quad (24)$$

then the radial polarization current can be written as

$$(1 - \rho_i^2 \nabla_\perp^2) j_r = j_r - \rho_i^2 \frac{\partial}{\partial r} \left[\frac{1}{r} \frac{\partial}{\partial r} (r j_r) \right]. \quad (25)$$

Here ρ_i' is just the ion gyroradius if the Padé approximation (23) is assumed or the form given by the coefficient of the Laplacian operator in Eq. (22) under the approximations given there. Putting Eqs. (12), (17), (19), and (25) together we arrive at an equation for the magnetic perturbation,

$$\begin{aligned} \frac{\partial}{\partial r} \left[\lambda'^2 \frac{1}{r} \frac{\partial}{\partial r} (r B_\varphi) \right] - \frac{k_\parallel^2 V_A^2}{\omega^2} \rho_i'^2 \frac{\partial}{\partial r} \left[\frac{1}{r} \frac{\partial}{\partial r} (r B_\varphi) \right] \\ + \left(\frac{k_\parallel^2 V_A^2}{\omega^2} - 1 \right) B_\varphi = 0, \end{aligned} \quad (26)$$

where we have written $V_A'^2 = V_A^2 (1 - \omega^2/\Omega_i^2)$ to account for the finite frequency correction.

Next, let us consider the structure of modes in a system consisting of a piecewise constant density profile, with a constant density n_1 for distances $r < R$ and n_2 for $r > R$. We will also assume that the electron and ion temperatures are also piecewise constant and that the background magnetic field is uniform throughout. Then the coefficients in Eq. (26) are constant in each segment, and the equation can be written as

$$\frac{\partial}{\partial r} \left[\frac{1}{r} \frac{\partial}{\partial r} (r B_\varphi) \right] + \frac{k_\parallel^2 V_A'^2 / \omega^2 - 1}{\lambda'^2 - (k_\parallel^2 V_A'^2 / \omega^2) \rho_i'^2} B_\varphi = 0. \quad (27)$$

This equation can be cast into Bessel's equation

$$\frac{\partial^2 B_\varphi}{\partial r^2} + \frac{1}{r} \frac{\partial B_\varphi}{\partial r} + \left(\kappa^2 - \frac{1}{r^2} \right) B_\varphi = 0, \quad (28)$$

where, writing out all terms explicitly, the quantity κ^2 is given by

$$\begin{aligned} \frac{\rho^2}{\lambda^2} < \frac{\omega^2}{k_\parallel^2 V_A^2} < 1 \quad \text{for } \frac{\rho^2}{\lambda^2} < 1 \\ \text{or } \frac{\rho^2}{\lambda^2} > \frac{\omega^2}{k_\parallel^2 V_A^2} > 1 \quad \text{for } \frac{\rho^2}{\lambda^2} > 1, \end{aligned} \quad (32)$$

where the left inequality occurs in the cold plasma limit ($\beta < m_e/m_i$) and the right side corresponds to the warm plasma limit ($\beta > m_e/m_i$). Since the electron thermal speed $v_e^2 = T_e/m_e$ can be written as $v_e = V_A \rho_s / \lambda$, these inequalities indicate that in both regions the waves propagate for parallel phase velocities between the Alfvén speed and the electron thermal speed when the ion gyroradius correction is neglected. Including this correction, the square of the electron

thermal speed should be multiplied by $(1 + \rho_1'^2/\rho_s^2)$.

Solutions to Eq. (28) are of the form $AJ_1(\kappa r) + BY_1(\kappa r)$ for $\kappa^2 > 0$, corresponding to propagating solutions and $CI_1(\kappa r) + DK_1(\kappa r)$ in the evanescent case, $\kappa^2 < 0$. In this case we write $\kappa = \sqrt{|\kappa^2|}$. We apply the usual requirements that for the inner region, $B = D = 0$ so that the solution is regular at the origin and in the outer region, $C = 0$ in the evanescent case to prevent an infinite solution as $r \rightarrow \infty$. The solutions across the boundary must satisfy the boundary conditions that $\Delta B_\phi = 0$ and $\Delta E_z = 0$. By Eq. (17) this implies that the second boundary condition can be written as

$$\lambda_1'^2 \frac{1}{r} \frac{\partial}{\partial r} (rB_{\phi 1}) = \lambda_2'^2 \frac{1}{r} \frac{\partial}{\partial r} (rB_{\phi 2}). \quad (33)$$

To be more specific, let us assume that the inner region (called region 1) is a density cavity so that the Alfvén speed is higher in the inner region than in the outer region (region 2), so that $V_{A1} > V_{A2}$. So, considering the case where the wave is propagating in region 1 and evanescent in region 2 we have

$$B_{\phi 1} = AJ_1(\kappa_1 r), \quad B_{\phi 2} = DK_1(\kappa_2 r). \quad (34)$$

The equality of these two quantities implies $D/A = J_1(\kappa_1 R)/K_1(\kappa_2 R)$. Applying the boundary condition (33), we use the identity $J_1'(x) + J_1(x)/x = J_0(x)$ to write

$$\kappa_1 \lambda_1'^2 AJ_0(\kappa_1 R) = \kappa_2 \lambda_2'^2 DK_0(\kappa_2 R). \quad (35)$$

Combining these two boundary conditions gives

$$\kappa_1 \lambda_1'^2 J_0(\kappa_1 R) K_1(\kappa_2) - \kappa_2 \lambda_2'^2 J_1(\kappa_1 R) K_0(\kappa_2 R) = 0. \quad (36)$$

This equation must be solved as an eigenvalue problem for the parallel phase velocity $V = \omega/k_{\parallel}$, which is implicit in Eq. (36) through the definitions of λ'^2 following Eq. (17) and κ in Eq. (29) or the simplified version Eq. (30).

On the other hand, if the wave can propagate outside the inner region, the boundary conditions become

$$AJ_1(\kappa_1 R) = CJ_1(\kappa_2 R) + DY_1(\kappa_2 R) \quad (37)$$

and

$$\kappa_1 \lambda_1'^2 AJ_0(\kappa_1 R) = \kappa_2 \lambda_2'^2 [CJ_0(\kappa_2 R) + DY_0(\kappa_2 R)]. \quad (38)$$

Other than the overall normalization given by A , these two equations can be solved for C and D for any values of the coefficients. Thus, in this region there are a continuum of possible wave modes.

There are a number of possible combinations of parameters that give different combinations of propagating and evanescent modes based on the relative values of V_{A1} , V_{A2} , v_{e1} , and v_{e2} . (Remember that these parameters can be generalized to include finite frequency and ion gyroradius effects as indicated above.) Some examples of these combinations are shown in Fig. 4. In each panel of this figure, the dark line represents the Alfvén speed profile and the lighter line is the profile of the electron thermal speed. The left-hand side of each panel represents a cavity region (higher Alfvén speed) while the right-hand side is a region of enhanced density (low Alfvén speed). The dispersion relation given by Eq. (31) indicates that parallel phase velocities near the Alfvén

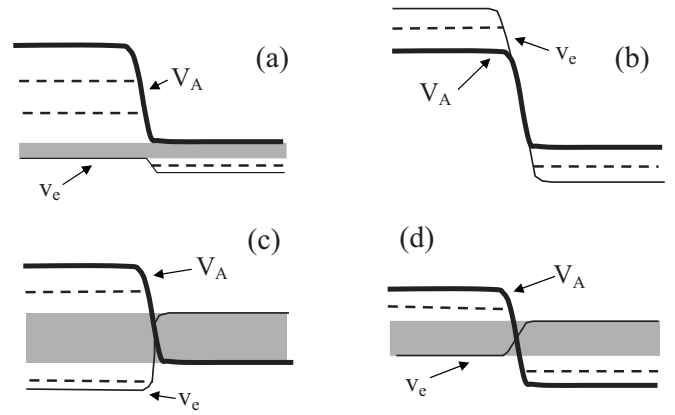


FIG. 4. Schematic diagrams of propagation regions for various types of interfaces. In each panel, the heavy solid line represents the Alfvén speed, and the lighter solid line represents the effective electron thermal velocity. Gray shaded areas indicate phase velocities in a continuum region that can propagate on both sides of the interface. Dashed lines indicate regions where discrete modes are possible. (a) Cold plasma on both sides of the interface (cf. Chaston *et al.*, Ref. 4). (b) Warm cavity in contact with a cold, dense region. (c) Cold cavity in contact with warmer dense region (cf. Vincena *et al.*, Ref. 27). (d) Cold cavity in contact with warm dense region, with parameters relevant to the lobe/plasma sheet interface.

speed correspond to low perpendicular wavenumber, while the parallel phase velocity approaches the electron thermal speed for large perpendicular wavenumber. The gray-shaded region indicates phase velocities for which propagation is possible on both sides of the interface and thus a continuum of states is possible, while dashed lines indicate regions in which discrete modes should be found. It should be emphasized that these diagrams qualitatively describe systems in a slab geometry as well as for the cylindrical geometry discussed quantitatively above. Cases illustrated in this figure are as follows:

1. Figure 4(a) shows a system in which $v_{e2} < v_{e1} < V_{A2} < V_{A1}$. In this case, the plasma is cold on both sides of the interface. Long perpendicular wavelength modes in the cavity cannot penetrate outside; however, shorter wavelength modes can. In contrast, the shorter perpendicular wavelength modes outside the cavity cannot go in. This scenario is representative of the results found by Chaston *et al.*,⁴ which show that the waves primarily trapped in the cavity.

2. Figure 4(b) shows the case where $v_{e2} < V_{A2} < V_{A1} < v_{e1}$, or a hot cavity surrounded by a cold denser region. In this situation, the allowable regions of parallel phase velocity are distinct on the two sides of the interface, and so no modes can propagate across the boundary. This situation may be realized at higher altitudes in the auroral zone where the hot plasma in the cavity has a thermal speed greater than the Alfvén speed.

3. Figure 4(c) illustrates a case with $v_{e1} < V_{A2} < v_{e2} < V_{A1}$. This diagram would apply for the parameters of the LAPD experiment given by Vincena *et al.*²⁷ with side 2 being in the central part of the device while side 1 is on the outside. For this structure, all of the kinetic Alfvén waves excited in region 2 are able to propagate into region 1, making this structure optimal for the purposes of Vincena *et al.*²⁷ who were investigating the propagation of the Alfvén wave

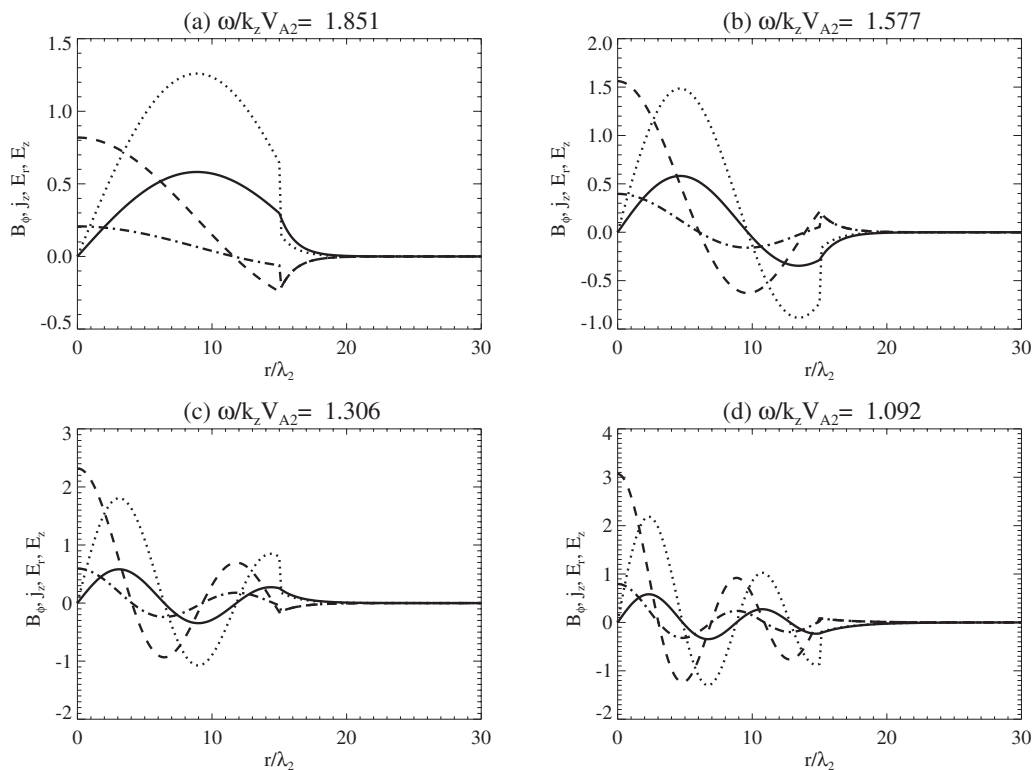


FIG. 5. Mode structures of the four discrete modes found in a plasma cavity with a sharp boundary at a radius of $15\lambda_2$ with $V_{A1}=2V_{A2}$, $\lambda_1=2\lambda_2$, $\rho_{s1}=\rho_{i1}=0.2\lambda_2$, and $\rho_{s2}=\rho_{i2}=0.1\lambda_2$, where the 1 and 2 subscripts correspond to inside and outside the cavity, respectively. In each panel, the solid curve gives B_ϕ , the dotted curve E_r , the dashed curve E_z , and the dashed-dotted curve j_z . The four panels give modes with parallel phase velocities of (a) 1.851, (b) 1.577, (c) 1.306, and (d) 1.092 of the outside Alfvén velocity. Discrete modes should occur between 1 and $2V_{A2}$ according to the arguments given in the text.

from the kinetic to the inertial regime. In this configuration, waves generated near the Alfvén speed in region 1 would not be able to penetrate into the central region of the plasma.

4. Figure 4(d) shows a case where $V_{A2} < v_{e1} < v_{e2} < V_{A1}$, i.e., a cold cavity surrounded by a hotter plasma. In a slab geometry, this case could correspond to the lobe/plasma sheet interface in the magnetotail. In this case, discrete modes are found at long perpendicular wavelength on both sides of the interface, while shorter perpendicular wavelength waves can propagate across the boundary.

The cases shown are not all-inclusive; however, these illustrate the qualitative behavior that is possible.

Finally, let us consider the structure of these modes. Consider the case shown in Fig. 4(a), corresponding to the auroral zone data of Chaston *et al.*⁴ Estimating the parameters for this case, the density in the cavity is about a factor of 4 below the outside region; thus the Alfvén speed in the cavity is about twice that outside. Since in this plasma the magnetic field is roughly constant, the inertial length inside is also twice that outside. While the temperature is difficult to measure, the plasma is cold on both sides, in the sense that the electron thermal velocity is less than the Alfvén speed. We will take the ion acoustic gyroradius to be 0.1 times the electron thermal speed in the outside region, and twice as large in the cavity. We also assume that the ion gyroradius term is equal to the ion acoustic gyroradius. Under these assumptions, there should be discrete modes with phase velocities between 1 and 2 times the outside Alfvén speed, and a continuum of modes between the outside Alfvén speed and

0.28 times that value. As in the discussion leading to Eqs. (36)–(38), we assume that the boundary between the two regions is a sharp discontinuity at a radius of 15 times the inertial length in the external region. Figures 5 and 6 show this situation. These figures show the wave magnetic field, field-aligned current, and the radial and parallel components of the electric field. In each panel of these figures, the solid curves are the magnetic field, the dashed-dotted curve is the field-aligned current, the dotted curve is the perpendicular field, and the dashed curve is the parallel electric field.

Figure 5 shows that four modes can be found in the appropriate phase velocity range, with the appropriate mode structure as the phase velocity is decreased. The magnetic field and the parallel electric field are continuous at the interface as required by Maxwell's equations, while the field-aligned current and perpendicular electric field show discontinuities. The scales of the fields are arbitrary, with a normalization of $A=1$ in the expressions given by Eqs. (34) and (37). The magnetic field has 1, 2, 3, and 4 nodes in each successive mode (including the node at 0), as would be expected. Figure 6 shows four examples of waves in the continuum region for arbitrary phase velocities in this region. The increase of the wavelength in the outside region can be clearly seen in these figures. In addition, the B_ϕ and E_z components can be seen to be 90° out of phase, indicating a standing wave. The relative amplitude of the wave outside the cavity is largest closer to the cutoff, and becomes smaller for smaller phase velocities.

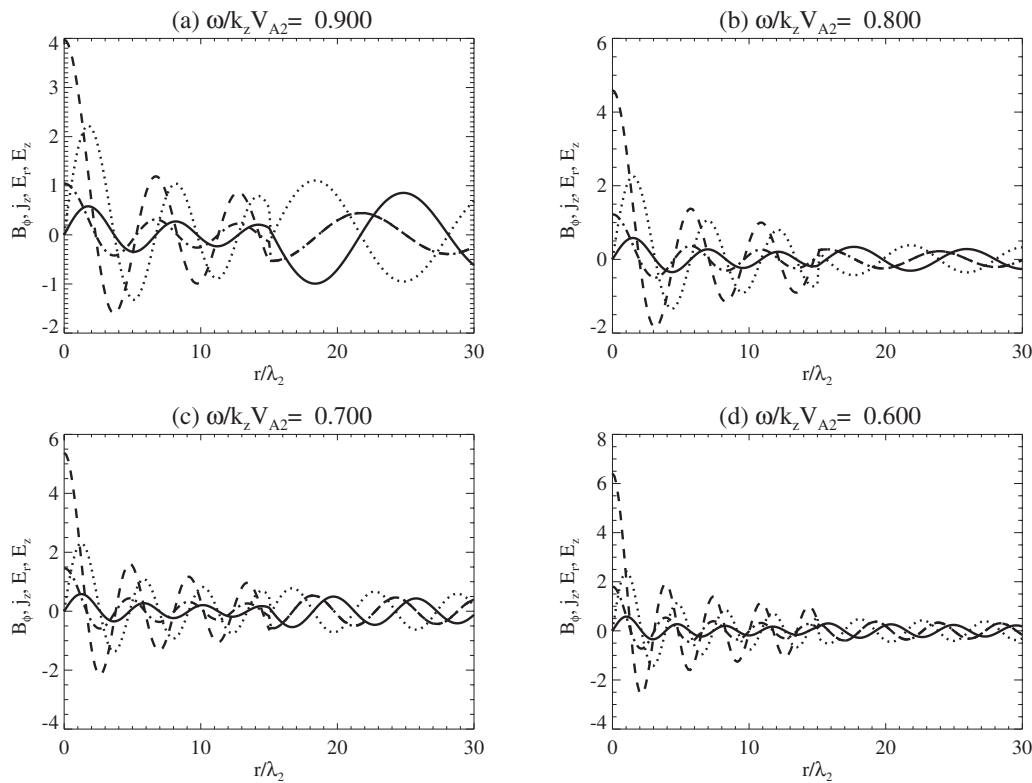


FIG. 6. Mode structure of four representative continuum modes for the same plasma parameters as in Fig. 5. The theory given in the text predicts a continuum band from 0.28 to 1 times of outside Alfvén speed. Plots are shown for modes with phase velocities of (a) 0.9, (b) 0.8, (c) 0.7, and (d) 0.6 of the outside Alfvén speed.

IV. CONCLUSIONS

These results illustrate the structure of the kinetic Alfvén wave dispersion relation in the presence of perpendicular gradients in the Alfvén speed and the effective electron thermal speed. Such interfaces are intrinsic to laboratory produced plasmas and are also ubiquitous in space plasmas. The kinetic Alfvén wave dispersion relation can be generalized to finite frequency and finite ion gyroradius effects by including corrections to the Alfvén speed, the electron inertial length and the ion gyroradius based on kinetic theory. These considerations give a basis for the two-fluid model frequently used based on the full kinetic dispersion relation. It is important to note that the formulation of the kinetic dispersion relation given by Lysak and Lotko¹⁵ and that given by Gekelman *et al.*²⁴ are in fact equivalent, and either may be used as is convenient for the specific application.

Being able to write the dispersion relation in a two-fluid form facilitates the generalization of the dispersion relation to inhomogeneous plasmas. Kinetic Alfvén waves propagate with parallel phase velocities between the Alfvén speed and the effective electron thermal speed, regardless of which of these speeds is larger. This consideration allows the use of relatively simple diagrams as in Fig. 4 in order to qualitatively determine the nature of Alfvén wave solutions on either side of an interface. Such diagrams may be useful in the interpretation of lab and space observations when measured parameters can be used to determine the relevant speeds on either side of the interface. While the work presented here considered a sharp interface between two uniform plasma

regions, future work will generalize this model to smooth transitions between regions with different plasma characteristics.

While the existence of discrete Alfvén wave modes in an inhomogeneous plasma is an important result, equally important is the evolution of Alfvén waves in inhomogeneous systems in time. Such a study using fluid simulations will be the focus of future work. This type of study can also consider the effect of parallel gradients in the Alfvén speed, which is particularly important in the context of the Earth's auroral zone, where such gradients lead to the so-called ionospheric Alfvén resonator.^{42–46} Understanding the dynamics of Alfvén waves in such plasmas with inhomogeneities in all possible direction will be a strong step forward in the understanding of magnetosphere-ionosphere coupling in the Earth's magnetosphere as well as in laboratory plasmas and other cosmic plasma situations, such as Jupiter's magnetosphere and the solar corona.

ACKNOWLEDGMENTS

This work has greatly benefited from discussions with Yan Song, Chris Chaston, and Walter Gekelman.

This research is supported in part by NSF Grant No. ATM-0613473.

APPENDIX: FINITE ION GYRORADIUS CORRECTIONS TO POLARIZATION CURRENT

We wish to find an expression for the polarization current which does not depend on the assumption of a given perpendicular wave number. As in the rest of the paper, we

will assume that the electric field is in the xz -plane and that the magnetic perturbation is in the y -direction. We will choose standard phase space variables for the plasma, in which the canonical coordinates are given by $\mathbf{q}=(z, \varphi, Y)$ and the corresponding momenta are $\mathbf{p}=(p_z, p_\varphi, qBX)$ where $p_\varphi = mv_\perp^2/2\Omega$ and the spatial coordinates are related to the canonical variables by

$$x = X - (v_\perp/\Omega)\cos\varphi, \quad y = Y + (v_\perp/\Omega)\sin\varphi, \quad (A1)$$

$$v_x = v_\perp \sin\varphi, \quad v_y = v_\perp \cos\varphi.$$

As usual, the parallel velocity is constant and thus the z coordinate changes linearly in time. In this case, the x -component of the current can be written as

$$\begin{aligned} \delta j_x &= (\mathbf{x}, t) \\ &= ne \int d^3q d^3p \delta[\mathbf{x} - \mathbf{x}(\mathbf{q}, \mathbf{p})] v_\perp \sin\varphi \delta f(\mathbf{q}, \mathbf{p}, t). \end{aligned} \quad (A2)$$

We can solve the Vlasov equation in the usual manner assuming the perturbation is turned on at $t=0$ to find

$$\begin{aligned} \delta f(\mathbf{q}, \mathbf{p}, t) &= -\frac{q}{m} \int_0^t dt' \left[(\delta E'_x - v_z \delta B'_y) \frac{\partial f_0}{\partial v'_x} \right. \\ &\quad \left. + (\delta E'_z + v'_x \delta B'_y) \frac{\partial f_0}{\partial v'_z} \right]. \end{aligned} \quad (A3)$$

In this expression, the primed variables are evaluated at the past time. For example, we can write

$$\delta E'_x = \delta E_x[x(t'), z(t'), t']. \quad (A4)$$

If we then assume a long parallel wavelength so that the z variations of the fields can be neglected, which is appropriate for the ions since the Alfvén speed is much greater than the ion thermal speed in a low- β plasma, and we note that the terms involving v_z and $\partial f_0/\partial v_z$ will vanish upon the integration in Eq. (A2) over p_z . The only term that will survive in Eq. (A3) is the first term involving $\delta E'_x$, then Eq. (A3) becomes

$$\delta f(\mathbf{q}, \mathbf{p}, t) = -\frac{q}{m} \int_0^t dt' \delta E_x[x(t'), t'] \sin\varphi' \frac{\partial f_0}{\partial v_\perp}, \quad (A5)$$

where we have set $\varphi' = \varphi - \Omega\tau$, with $\tau = t - t'$. Then using the delta functions to simplify the integral, Eq. (A2) becomes

$$\begin{aligned} \delta j_x(x, t) &= -\frac{ne^2}{m} \int d\varphi dv_z v_\perp dv_\parallel v_\perp \sin\varphi \frac{\partial f_0(v_\perp, v_z)}{\partial v_\perp} \\ &\quad \times \int_0^t dt' \delta E_x[X - (v_\perp/\Omega)\cos\varphi', t'] \sin\varphi'. \end{aligned} \quad (A6)$$

Here we have switched from considering f as being the phase space density in momentum space to it being the density in velocity space. In addition, we have written the dependence of the electric field out explicitly.

Next we expand the electric field about the guiding center position X ,

$$\delta E_x(x') = \delta E_x(X) - \frac{v_\perp}{\Omega} \cos\varphi' \frac{\partial \delta E_x}{\partial X} + \frac{v_\perp^2}{2\Omega^2} \cos^2\varphi' \frac{\partial^2 \delta E_x}{\partial X^2}, \quad (A7)$$

where again x' represents the position at time t' . However, we would really like to express this in terms of the present position x . To do this we expand $\delta E_x(X)$ about the position x ,

$$\delta E_x(X) = \delta E_x(x) + \frac{v_\perp}{\Omega} \cos\varphi \frac{\partial \delta E_x}{\partial x} + \frac{v_\perp^2}{2\Omega^2} \cos^2\varphi \frac{\partial^2 \delta E_x}{\partial x^2}. \quad (A8)$$

Doing a similar expansion for the derivative terms, we find that

$$\begin{aligned} \delta E_x(x') &= \delta E_x(x) + \frac{v_\perp}{\Omega} (\cos\varphi - \cos\varphi') \frac{\partial \delta E_x}{\partial x} \\ &\quad + \frac{v_\perp^2}{2\Omega^2} (\cos\varphi - \cos\varphi')^2 \frac{\partial^2 \delta E_x}{\partial x^2}. \end{aligned} \quad (A9)$$

Using a Maxwellian for the distribution function, Eq. (A6) can then be written as

$$\begin{aligned} \delta j_x &= \frac{2ne^2}{\pi ma^4} \int_0^\infty v_\perp^2 dv_\perp e^{-v_\perp^2/a^2} \int_0^t dt' \\ &\quad \times \left\{ \delta E_x(x, t') \int_0^{2\pi} d\varphi \sin\varphi \sin\varphi' \right. \\ &\quad + \frac{v_\perp}{\Omega} \frac{\partial \delta E_x(x, t')}{\partial x} \int_0^{2\pi} d\varphi \sin\varphi \sin\varphi' (\cos\varphi - \cos\varphi') \\ &\quad + \frac{v_\perp^2}{2\Omega^2} \frac{\partial^2 \delta E_x(x, t')}{\partial x^2} \int_0^{2\pi} d\varphi \sin\varphi \sin\varphi' (\cos\varphi \\ &\quad \left. - \cos\varphi')^2 \right\}. \end{aligned} \quad (A10)$$

Here we write $\sin\varphi' = \sin(\varphi - \Omega\tau) = \sin\varphi \cos\Omega\tau - \cos\varphi \sin\Omega\tau$ and similarly for $\cos\varphi'$. Using these expressions, the angular integrals in Eq. (A10) can be done, which results in the first derivative term vanishing (since there are an odd number of trig functions in each integral). This leads to

$$\begin{aligned} \delta j_x(x, t) &= \frac{ne^2}{ma^4} \int_0^\infty v_\perp^3 dv_\perp e^{-v_\perp^2/a^2} \int_0^t dt' \left[2\delta E_x(x, t') \cos\Omega\tau \right. \\ &\quad \left. + \frac{v_\perp^2}{2\Omega^2} \frac{\partial^2 \delta E_x}{\partial x^2} (\cos\Omega\tau - \cos 2\Omega\tau) \right]. \end{aligned} \quad (A11)$$

Now we can take the inverse Laplace transform (written in terms of frequency) in order to perform the integral over past times in the usual manner by assuming a vanishing small positive imaginary part to the frequency,

$$\delta j_x(\omega) = \int_0^\infty dt e^{i\omega t} \delta j_x(t). \quad (A12)$$

Then, for example, the first term in the brackets of Eq. (A11) can be evaluated by switching the order of the t and t' integrations, leading to terms of the form,

$$\begin{aligned}
& \int_0^\infty dt \int_0^t dt' e^{i\omega t'} \delta E_x(t') \cos \Omega(t-t') \\
&= \int_0^\infty dt' \delta E_x(t') \int_{t'}^\infty dt \frac{1}{2} e^{i\omega t} [e^{i\Omega(t-t')} + e^{-i\Omega(t-t')}] \\
&= \int_0^\infty dt' \delta E_x(t') \frac{i}{2} e^{i\omega t'} \left(\frac{1}{\omega + \Omega} - \frac{1}{\omega - \Omega} \right) \\
&= \delta E_x(\omega) \frac{i\omega}{\omega^2 - \Omega^2}. \tag{A13}
\end{aligned}$$

Similarly, the $\cos 2\Omega\tau$ term will give an expression with a denominator of $\omega^2 - 4\Omega^2$. Putting these together and performing the velocity integrals in Eq. (A11) leads to the result

$$\begin{aligned}
\delta j_x(x, \omega) = & -\frac{i\omega e^2}{\Omega^2} \left\{ \frac{1}{1 - \omega^2/\Omega^2} \delta E_x(\omega) \right. \\
& \left. + \rho_i^2 \left[\frac{1}{1 - \omega^2/\Omega^2} - \frac{1}{4(1 - \omega^2/4\Omega^2)} \right] \frac{\partial^2 \delta E_x}{\partial x^2} \right\}, \tag{A14}
\end{aligned}$$

where $\rho_i^2 = a^2/2\Omega^2$ is the thermal ion gyroradius. This can be conveniently rewritten in the form,

$$\begin{aligned}
\delta j_x(x, \omega) = & \frac{-i\omega}{\mu_0 V_A^2 (1 - \omega^2/\Omega^2)} \left[\delta E_x(x, \omega) \right. \\
& \left. + \frac{3\rho_i^2}{4(1 - \omega^2/4\Omega^2)} \frac{\partial^2 \delta E_x}{\partial x^2} \right]. \tag{A15}
\end{aligned}$$

This expression is quoted above as Eq. (21).

- ¹C. C. Chaston, C. W. Carlson, R. E. Ergun, and J. P. McFadden, *Phys. Scr.* **T84**, 64 (2000).
- ²C. C. Chaston, J. W. Bonnell, L. M. Peticolas, C. W. Carlson, J. P. McFadden, and R. E. Ergun, *Geophys. Res. Lett.* **29**, 1535 (2002).
- ³C. C. Chaston, J. W. Bonnell, C. W. Carlson, J. P. McFadden, R. E. Ergun, and R. J. Strangeway, *J. Geophys. Res.* **108**, 8003 (2003).
- ⁴C. C. Chaston, V. Genot, J. W. Bonnell, C. W. Carlson, J. P. McFadden, R. E. Ergun, R. J. Strangeway, E. J. Lund, and K. J. Hwang, *J. Geophys. Res.* **111**, A03206 (2006).
- ⁵J. R. Wygant, A. Keiling, C. A. Cattell, M. Johnson, R. L. Lysak, M. Temerin, F. S. Mozer, C. A. Kletzing, J. D. Scudder, W. Peterson, C. T. Russell, G. Parks, M. Brittacher, G. Germany, and J. Spann, *J. Geophys. Res.* **105**, 18675 (2000).
- ⁶J. R. Wygant, A. Keiling, C. A. Cattell, R. L. Lysak, M. Temerin, F. S. Mozer, C. A. Kletzing, J. D. Scudder, V. Streltsov, W. Lotko, and C. T. Russell, *J. Geophys. Res.* **107**, 1201 (2002).
- ⁷A. Keiling, J. R. Wygant, C. Cattell, W. Peria, G. Parks, M. Temerin, F. S. Mozer, C. T. Russell, and C. A. Kletzing, *J. Geophys. Res.* **107**, 1132 (2002).
- ⁸A. Keiling, J. R. Wygant, C. A. Cattell, F. S. Mozer, and C. T. Russell, *Science* **299**, 383 (2003).

- ⁹A. Keiling, G. K. Parks, J. R. Wygant, J. Dombeck, F. S. Mozer, C. T. Russell, A. V. Streltsov, and W. Lotko, *J. Geophys. Res.* **110**, A10S11 (2005).
- ¹⁰A. Hasegawa, *J. Geophys. Res.* **81**, 5083 (1976).
- ¹¹C. K. Goertz and R. W. Boswell, *J. Geophys. Res.* **84**, 7239 (1979).
- ¹²R. L. Lysak and C. T. Dum, *J. Geophys. Res.* **88**, 365 (1983).
- ¹³C. A. Kletzing, *J. Geophys. Res.* **99**, 11095 (1994).
- ¹⁴B. J. Thompson and R. L. Lysak, *J. Geophys. Res.* **101**, 5359 (1996).
- ¹⁵R. L. Lysak and W. Lotko, *J. Geophys. Res.* **101**, 5085 (1996).
- ¹⁶R. L. Lysak, *Geophys. Res. Lett.* **25**, 2089 (1998).
- ¹⁷V. T. Tikhonchuk and R. Rankin, *Phys. Plasmas* **7**, 2630 (2000).
- ¹⁸V. T. Tikhonchuk and R. Rankin, *J. Geophys. Res.* **107**, 1104 (2002).
- ¹⁹R. L. Lysak and Y. Song, *J. Geophys. Res.* **108**, 8005 (2003a).
- ²⁰R. L. Lysak and Y. Song, *J. Geophys. Res.* **108**, 1327 (2003b).
- ²¹R. L. Lysak and Y. Song, *J. Geophys. Res.* **110**, A10S06 (2005).
- ²²C. E. J. Watt, R. Rankin, and R. Marchand, *Phys. Plasmas* **11**, 1277 (2004).
- ²³W. Gekelman, H. Pfister, Z. Lucky, J. Bamber, D. Leneman, and J. Maggs, *Rev. Sci. Instrum.* **62**, 2875 (1991).
- ²⁴W. Gekelman, S. Vincena, D. Leneman, and J. Maggs, *J. Geophys. Res.* **102**, 7225 (1997).
- ²⁵C. A. Kletzing, S. R. Bounds, J. Martin-Hiner, W. Gekelman, and C. Mitchell, *Phys. Rev. Lett.* **90**, 035004 (2003).
- ²⁶J. E. Maggs and G. J. Morales, *Geophys. Res. Lett.* **23**, 633 (1996).
- ²⁷S. Vincena, W. Gekelman, and J. Maggs, *Phys. Rev. Lett.* **93**, 105003 (2004).
- ²⁸A. M. Persoon, D. A. Gurnett, W. K. Peterson, J. H. Waite, J. L. Burch, and J. L. Green, *J. Geophys. Res.* **93**, 1871 (1988).
- ²⁹A. I. Eriksson, B. Holback, P. O. Dovner, R. Boström, G. Holmgren, M. André, L. Eliasson, and P. M. Kintner, *Geophys. Res. Lett.* **21**, 1843 (1994).
- ³⁰R. Lundin, L. Eliasson, G. Haerendel, M. Boehm, and B. Holback, *Geophys. Res. Lett.* **21**, 1903 (1994).
- ³¹R. J. Strangeway, L. Kepko, R. C. Elphic, C. W. Carlson, R. E. Ergun, J. P. McFadden, W. J. Peria, G. T. Delory, C. C. Chaston, M. Temerin, C. A. Cattell, E. Möbius, L. M. Kistler, D. M. Klumpar, W. K. Peterson, E. G. Shelley, and R. F. Pfaff, *Geophys. Res. Lett.* **25**, 2065 (1998).
- ³²R. Rankin, J. C. Samson, V. T. Tikhonchuk, and I. Voronkov, *J. Geophys. Res.* **104**, 4399 (1999).
- ³³R. Rankin, R. Marchand, J. Y. Lu, K. Kabin, and V. T. Tikhonchuk, *Geophys. Res. Lett.* **32**, L05102 (2005).
- ³⁴T. Drozdenko and G. J. Morales, *Phys. Plasmas* **7**, 823 (2000).
- ³⁵V. Génot, P. Louarn, and D. LeQuéau, *J. Geophys. Res.* **104**, 22649 (1999).
- ³⁶V. Génot, P. Louarn, and F. Mottez, *J. Geophys. Res.* **105**, 27611 (2000).
- ³⁷V. Génot, F. Mottez, and P. Louarn, *Phys. Chem. Earth, Part C, Sol.-Terr. Planet. Sci.* **26**, 219 (2001).
- ³⁸V. Génot, P. Louarn, and F. Mottez, *Ann. Geophys.* **22**, 2081 (2004).
- ³⁹K. Rönmark, *Plasma Phys.* **23**, 699 (1983).
- ⁴⁰J. R. Johnson and C. Z. Cheng, *Geophys. Res. Lett.* **24**, 1423 (1997).
- ⁴¹A. Streltsov, W. Lotko, J. R. Johnson, and C. Z. Cheng, *J. Geophys. Res.* **103**, 26559 (1998).
- ⁴²S. V. Polyakov and V. O. Rapoport, *Geomagn. Aeron.* **21**, 816 (1981).
- ⁴³Y. Yu. Trakhtengertz and A. Ya. Feldstein, *Planet. Space Sci.* **32**, 127 (1984).
- ⁴⁴Y. Yu. Trakhtengertz and A. Ya. Feldstein, *J. Geophys. Res.* **96**, 19363 (1991).
- ⁴⁵R. L. Lysak, *J. Geophys. Res.* **96**, 1553 (1991).
- ⁴⁶R. L. Lysak, "Generalized model of the ionospheric Alfvén resonator," in *Auroral Plasma Dynamics*, edited by R. L. Lysak, AGU Monograph 80, p. 121 (1993).